JOURNAL OF ENVIRONMENTAL SCIENCES 77 (2019) 85–96

Available online at www.sciencedirect.com

ScienceDirect

www.elsevier.com/locate/jes

JES JOURNAL OF ENVIRONMENTAL SCIENCES

www.jesc.ac.cn

Thermodynamic prediction and experimental investigation of short-term dynamic membrane formation in dynamic membrane bioreactors: Effects of sludge properties

Zhenzhen Yu[1], *Yisong Hu*[1,3], *Mawuli Dzakpasu*[3], *Xiaochang C. Wang*[1,2,3,*]

1. *Key Lab of Northwest Water Resource, Environment and Ecology, MOE, Xi'an University of Architecture and Technology, Xi'an 710055, China*
2. *Key Lab of Environmental Engineering, Shaanxi Province, Xi'an 710055, China*
3. *International Science & Technology Cooperation Center for Urban Alternative Water Resources Development, Xi'an 710055, China*

ARTICLE INFO

Article history:
Received 6 March 2018
Revised 22 June 2018
Accepted 22 June 2018
Available online 30 June 2018

Keywords:
Dynamic membrane bioreactor
Dynamic membrane formation
XDLVO theory
Sludge properties
Wastewater treatment

ABSTRACT

In dynamic membrane bioreactors (DMBRs), a dynamic membrane (DM) forms on a support material to act as the separation membrane for solids and liquids. In this study, batch filtration tests were carried out in a DMBR using nylon mesh (25 μm) as support material to filtrate sludge suspensions of variable properties from three different sources to evaluate the effects on the short-term DM formation process (within 240 min). Furthermore, the extended Derjaguin–Landau–Verwey–Overbeek (XDLVO) theory was applied to analyze the sludge adhesion and cohesion behaviors on the mesh surface to predict quantitative parameters of the short-term DM formation process (including initial formation and maturation stage). The filtration results showed that the order of the initial DM formation time (permeate turbidity <1 NTU as an indicator) was as follows: sludge with poor settleability and dewaterability < normal sludge < sludge with poor flocculability. Moreover, normal sludge (regarding settleability, dewaterability, flocculability, and extracellular polymeric substance) showed a more acceptable DM formation performance (short DM formation time, low permeate turbidity, and high permeate flux) than sludge with poor settleability, dewaterability and flocculability. The influence of sludge properties on the initial DM formation time corroborates the prediction of sludge adhesion behaviors by XDLVO theory. Additionally, the XDLVO calculation results showed that acid–based interaction, energy barrier, and secondary energy minimum were important determinants of the sludge adhesion and cohesion behaviors. Therefore, short-term DM formation process may be enhanced to achieve stable long-term DMBR operation through positive modification of the sludge properties.

Introduction

Conventional membrane bioreactors (MBRs) are prevailingly challenged by membrane fouling, which is primarily caused by the deposited cake layer on the membrane surface (Ouyang and Liu, 2009; Yu et al., 2017). Although the deposited cake layer decreases the membrane flux, it, however, increases the rejection of fine particles, which is beneficial for improving the membrane

* *Corresponding author. E-mail:* xcwang@xauat.edu.cn (Xiaochang C. Wang).

https://doi.org/10.1016/j.jes.2018.06.017
1001-0742 © 2018 The Research Center for Eco-Environmental Sciences, Chinese Academy of Sciences. Published by Elsevier B.V.

process performance. Based on this advantage, dynamic membrane bioreactors (DMBRs) emerged as the alternative to the conventional MBRs. In DMBRs, a dynamic membrane (DM) layer can be formed on the surface of inexpensive support materials with comparatively larger pores (*e.g.*, mesh, woven fabrics, nonwoven fabric) when filtering suspended solid particles such as sludge flocs, colloids, and microbial cells (Fan and Huang, 2002; Kuberkar and Davis, 2000).

The DM layer effectively acts as the separation membrane rather than the support material itself (Park et al., 2004). The quick formation of a stable DM layer is critical for the DMBR operation to minimize poor quality effluents in the initial filtration stage due to the passage of suspended solids through the coarse pores of the support material. The DMBR process operation involves three stages (Hu et al., 2016): DM layer formation, stable filtration, and cleaning for DM regeneration. The DM layer formation could be further divided into the initial DM formation stage (less than 5 min) and DM maturation stage (approximately 240 min). The macroscopic indicator of the initial DM formation is a sharp reduction of permeate turbidity (<1 NTU) along with a drastic decrease of permeate flux. The DM maturation stage is characterized by a continuous decrease of the permeate turbidity, a reduction of the permeate flux and an increase of the filtration resistance (Hu et al., 2016). Moreover, it is reported that the interactions of membrane–foulant and foulant–foulant controlled the different filtration stages in the ultrafiltration membrane filtration (Wang et al., 2013a). Similarly, during the initial DM formation stage, the sludge flocs in the DMBR deposit on the clean membrane surface. This process is dominated by the interactions between the membrane and sludge flocs and is defined as sludge adhesion behaviors (adhesion process). Conversely, at the DM maturation stage, most of the membrane surface area is covered with sludge flocs, and consequently, the interactions between the approaching sludge flocs and the deposited sludge flocs predominately replace the membrane–sludge floc interactions to control the subsequent formation of the DM layer. Accordingly, these sludge floc–sludge floc interactions are defined as sludge cohesion behaviors (cohesion process).

From the force point of view, the formation of the cake layer can be described as a dynamic process under hydrodynamic and thermodynamic forces (Hong et al., 2013). The dominant hydrodynamic forces include the permeate drag force, inertial lift force, shear force, and net gravity force. In contrast, the thermodynamic forces are presented by the physicochemical interactions in the short distance between the membrane surface and foulants, which consist of Lifshitz–van der Waals (LW), Lewis acid–base (AB), and electrostatic double layer (EL) interactions as described by the extended Derjaguin–Landau–Verwey–Overbeek (XDLVO) theory (Lin et al., 2014a). In general, the permeate drag force which is induced by membrane flux (filtration pressure) could transport the sludge flocs towards the support material surface. The total forces (XDLVO force) of LW, AB and EL force generally tend to be attractive (Hong et al., 2013), which could be responsible for the attachment of the sludge flocs to the support material surface. The microcosmic force analysis of a sludge floc very close to the support material surface is shown in Appendix A Fig. S1. In DMBRs the very high membrane flux (permeate drag force) at the very beginning induced the sludge flocs rapidly approaching to the support material surface in a quite short period, which affect the long-distance movement of particles but not short-distance interaction between support material and particles, thus permeate drag force was not considered. The XDLVO force (thermodynamic forces) indeed caused the attachment of particles onto the support material surface, which play a role in the stability of the adhesion behavior over a long period except for the very initial filtration stage. Thus, in this paper the XDLVO force was focused.

Recently, many researchers have successfully applied the XDLVO theory to quantitatively elucidate the membrane–foulant and/or foulant–foulant interactions for the membrane fouling in the conventional membrane technology. For instance, Brant and Childress (2002) assessed the short-range interactions of membrane–colloids and colloids–colloids using the XDLVO theory and predicted different colloid fouling behaviors on the reverse osmosis (RO) membranes. Furthermore, Hongjun Lin's group extended the applications of the XDLVO theory to analyze the interactions between the membrane surface and sludge flocs in MBRs (Cai et al., 2017; Hong et al., 2013). The findings indicated that a repulsive energy barrier existed during the process of sludge floc attachment onto both the clean and sludge floc-modified membrane surfaces. Overall, these findings demonstrate that the XDLVO theory can be used to analyze short-range interactions between membrane surfaces and sludge flocs in MBRs (Shen et al., 2015). However, most of the studies in MBRs have not clearly distinguished the different roles of adhesion behaviors between membrane and foulants and cohesion behaviors between foulants and foulants on the membrane fouling. The discussion of this aspect on the dynamic membrane filtration is even less.

As indicated above, DMBR is a promising substitute to the MBR. Thus, it is conceivable that there are no significant differences in the sludge properties of the two bioreactors. However, the coarse-pore support materials (10–200 μm) used in DMBRs are notably different from those used in MBRs with smaller pore sizes (<1 μm), resulting in different sludge filtration behaviors. To the best of our knowledge, the prediction of the adhesion and cohesion behaviors of sludge flocs in the DM formation process in DMBRs is rarely reported. Application of the XDLVO theory in this regard will contribute to elucidate the roles of sludge adhesion and cohesion behaviors in the different stages of DM formation. Moreover, it can provide useful information to improve the understanding and control of the DM layer formation process in DMBRs.

On the other hand, for a given membrane and operational condition, the properties of the sludge suspension significantly affect the DM formation process. Several studies have proposed that the sludge morphology, settleability, dewaterability, flocculability, hydrophobicity/hydrophilicity, and extracellular polymeric substances (EPS) are the factors that may be affecting the performance of the DM layer in DMBRs (Hu et al., 2016; Liang et al., 2013; Zhang et al., 2011), but further investigation is needed. In addition, combining the XDLVO theory with the practical DMBR operation verified that the XDLVO theory was suitable for predicting the formation and control process of the DM layer, which can provide useful guidelines for the enhancement of sludge properties and facilitate the stable operation of the DMBR system.

The objectives of this study were (1) to measure various surface parameters (such as zeta potential and contact angle) of different sludge samples and membrane, and theoretically predict the adhesion and cohesion behaviors of sludge flocs during the DM layer formation process using the XDLVO theory; (2) to carry out batch filtration tests to analyze the DM formation process and filtration behaviors using different sludge samples in a DMBR, and then evaluate the feasibility of using the XDLVO theory to predict the DM layer formation; and (3) to further analyze the effects of sludge properties on the DM layer formation process. Noteworthily, the first stage of DMBR process operation (DM layer formation concluding initial DM formation stage and DM maturation stage) critically affects the retention effect and plays an important role in the long-term stable operation. Thus, in this study the first stage was mainly emphasized by conducting short-term filtration tests. The "formation" for the DMBR refers to "short-term DM formation".

1. Materials and methods

1.1. Experimental DMBR apparatus and filtration tests

A lab-scale DMBR with a total effective volume of 30 L (30 cm × 21 cm × 47 cm), which was located at a full-scale wastewater treatment plant (WWTP) in Xi'an, China, was used in this study. As shown in Fig. 1, one flat-sheet DM module with a double-sided effective filtration area of 0.04 m^2 was vertically inserted between two baffle frames. The DM module was made of polyvinyl chloride plates and two layers of meshes. A nylon mesh with an equivalent aperture of 25 μm was used as the outer support layer. The inner layer was a stainless steel mesh with 5 mm pore size. The specific configuration of the DM module is illustrated in Appendix A Fig. S2. Air diffusers were placed at the bottom left and right corners of the reactor to continuously create aeration and circulation flow (30 L/min). The dissolved oxygen (DO) concentration in the reactor was in the range of 4 to 6 mg/L. An electric heater was used to control the temperature of the reactor at 20 ± 1 °C. Raw domestic wastewater was fed into the DMBR using a submersible pump controlled by a water level sensor. The quality of the wastewater is as following (average one ± standard deviation, n = 10): turbidity 79.1 ± 28.0 NTU, chemical oxygen demand (COD) 108.7 ± 53.9 mg/L, total nitrogen (TN) 37.3 ± 4.9 mg/L, ammonia (NH_3-N) 34.1 ± 1.8 mg/L, nitrate nitrogen (NO_3-N) 0.9 ± 0.3 mg/L, and total phosphorus (TP) 4.0 ± 0.7 mg/L. The DMBR was operated under the constant pressure mode by gravity flow, and the effluent was withdrawn continuously by a 10-cm water level difference between the bioreactor and the effluent port, thus suction pump and associated energy consumption were not needed for high-flux operation.

In this work, three kinds of activated sludge samples (sludges A, B, and C) were taken from the aeration tanks of the local WWTP and two lab-scale DMBRs that were installed at the local WWTP, respectively. Batch filtration tests were carried out within 240 min for the three kinds of sludge, according to the DM formation performance reported by Hu et al. (2016). Within a short filtration period (4 hr), the changes of sludge properties were considered to be negligible. Before the filtration, the mixed liquid suspended solids (MLSS) concentration of each sludge sample was adjusted to 2800 ± 150 mg/L with its supernatant to exclude the influence of MLSS on the permeate flux. The properties of the adjusted sludge samples were characterized including supernatant turbidity, sludge volume index (SVI), particle size distribution (PSD), capillary suction time (CST), normalized CST, and extracellular polymeric substances (EPS_{tot}) comprised of proteins (EPS_p) and carbohydrates (EPS_c) (Table 1). Each property was measured at least three times for every sludge sample. Subsequently, the prepared sludge was put into the DMBR. Under the constant pressure operation mode (10 cm water head), a reduction of permeate flux with operating time was observed, which was accompanied by a similar decrease of permeate turbidity. The filtration tests were performed three times for each sludge sample, and the representative data are reported.

1.2. XDLVO approach

The total surface tension parameter (γ^{Tol}) of a material can be calculated as the sum of an LW (γ^{LW}) and an AB (γ^{AB}) component of surface tension (van Oss et al., 1986):

$$\gamma^{Tol} = \gamma^{LW} + \gamma^{AB} \quad (1)$$

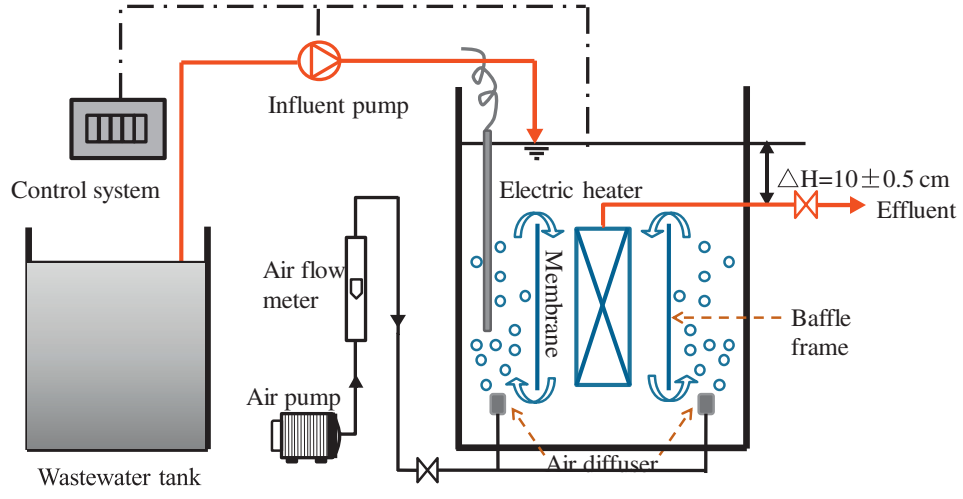

Fig. 1 – Dynamic membrane bioreactor (DMBR) apparatus of batch filtration test for evaluating DM formation.

Table 1 – Sludge properties of three kinds of sludge samples.

Parameters	Sludge A *	Sludge B *	Sludge C *
Supernatant turbidity (NTU)	1.63 ± 0.32	2.11 ± 0.45	31.70 ± 1.41
PSD (μm)	22.58 ± 0.91	38.27 ± 1.11	60.41 ± 3.44
SVI (mL/g)	246.98 ± 3.68	115.95 ± 5.73	68.33 ± 2.89
CST (sec)	49.35 ± 1.06	18.20 ± 3.82	23.33 ± 1.38
Normalized CST (sec L/g SS)	17.75 ± 0.38	7.65 ± 1.60	8.13 ± 0.48
EPS_p (mg/g SS)	77.46 ± 0.09	56.63 ± 0.76	53.26 ± 1.37
EPS_c (mg/g SS)	36.89 ± 1.62	13.72 ± 0.27	35.74 ± 2.40
EPS_{tot} (mg/g SS)	114.34 ± 1.71	70.35 ± 1.03	89.00 ± 3.78

PSD: particle size distribution; SVI: sludge volume index; CST: capillary suction time; EPS: extracellular polymeric substance.
* Value was given as average one ± standard deviation, $n = 3$.

where the polar γ^{AB} consists of non-additive electron donor (γ^-) and electron acceptor (γ^+) parameters as shown in Eq. (2) (van Oss and Good, 1988):

$$\gamma^{AB} = 2\sqrt{\gamma^+\gamma^-} \tag{2}$$

The surface tension parameters of a solid surface can be determined from the extended Young's equation, which relates the contact angle of a liquid on a solid surface to the solid surface tension parameters (γ^{LW}, γ^+, γ^-) of both the solid and the liquid (Bouchard et al., 1997):

$$(1+\cos\theta)\gamma_l^{Tol} = 2\left(\sqrt{\gamma_l^{LW}\gamma_s^{LW}} + \sqrt{\gamma_l^-\gamma_s^+} + \sqrt{\gamma_l^+\gamma_s^-}\right) \tag{3}$$

where θ is the contact angle. The subscripts l and s represent the liquid and solid surface. The surface tension parameters of solids such as the membrane surface (γ_m^{LW}, γ_m^+, γ_m^-) and sludge flocs (γ_s^{LW}, γ_s^+, γ_s^-) can be determined through a set of three Young's equations by measurements of the contact angles using three different probe liquids (ultrapure water, glycerol, and diiodomethane) with known surface tension parameters (γ_l^{Tol}, γ_l^{LW}, γ_l^+, γ_l^-). The surface thermodynamic parameters of the three probe liquids used in this study refer to a previous study (van Oss, 1995).

The free energy of adhesion per unit area ($\Delta G_{d_0}^{LW}$, $\Delta G_{d_0}^{AB}$, $\Delta G_{d_0}^{EL}$) represents the interaction energy per unit area between two infinite planar surfaces that are brought into contact, which is given by Eqs. (4)–(6), respectively (Hong et al., 2013; van Oss, 1995).

$$\Delta G_{d_0}^{LW} = -2\left(\sqrt{\gamma_m^{LW}}-\sqrt{\gamma_w^{LW}}\right)\left(\sqrt{\gamma_s^{LW}}-\sqrt{\gamma_w^{LW}}\right) \tag{4}$$

$$\Delta G_{d_0}^{AB} = 2\left[\sqrt{\gamma_w^+}\left(\sqrt{\gamma_s^-}+\sqrt{\gamma_m^-}-\sqrt{\gamma_w^-}\right)+\sqrt{\gamma_w^-}\left(\sqrt{\gamma_s^+}+\sqrt{\gamma_m^+}-\sqrt{\gamma_w^+}\right) -\sqrt{\gamma_s^-\gamma_m^+}-\sqrt{\gamma_s^+\gamma_m^-}\right] \tag{5}$$

$$\Delta G_{d_0}^{EL} = \frac{\varepsilon_0\varepsilon_r\kappa}{2}\left(\xi_s^2+\xi_m^2\right)\left[1-\coth(\kappa d_0)+\frac{2\xi_s\xi_m}{\xi_s^2+\xi_m^2}\,\mathrm{csch}(\kappa d_0)\right] \tag{6}$$

where γ^{LW}, γ^+, and γ^- are the surface thermodynamic parameters of the membrane (subscript m), water (subscript w) and sludge (subscript s). $\varepsilon_0\varepsilon_r$ is the permittivity of the suspending liquid. ξ is the surface zeta potential of the membrane (subscript m) and sludge flocs (subscript s). d_0 is the minimum equilibrium cut-off distance and is usually assigned a value of 0.158 nm (±0.009 nm). κ is the reciprocal Debye screening length, which can be calculated by Eq. (7):

$$\kappa = \sqrt{\frac{e^2\sum n_i z_i^2}{\varepsilon_0\varepsilon_r kT}} \tag{7}$$

where k is Boltzmann's constant, T is the temperature, e is the electron charge, n_i is the number concentration of ion i in solution and z_i is the valence of ion i.

The total adhesion free energy per unit area (ΔG_{swm}^{TOT}) between membrane and sludge is as indicated in Eq. (8) by the XDLVO theory:

$$\Delta G_{swm}^{TOT} = \Delta G_{d_0}^{LW} + \Delta G_{d_0}^{AB} + \Delta G_{d_0}^{EL} \tag{8}$$

Additionally, ΔG_{sws} signifies the free energy of interaction between two identical solid surfaces (subscript s) immersed in water (subscript w), which can be used to evaluate the surface hydrophobicity/hydrophilicity (van Oss, 2003). ΔG_{sws} is described as the following Eq. (9):

$$\Delta G_{sws} = -2\left(\sqrt{\gamma_s^{LW}}-\sqrt{\gamma_w^{LW}}\right)^2 - 4\left(\sqrt{\gamma_s^+\gamma_s^-}+\sqrt{\gamma_w^+\gamma_w^-}-\sqrt{\gamma_s^+\gamma_w^-}-\sqrt{\gamma_s^-\gamma_w^+}\right) \tag{9}$$

If $\Delta G_{sws} < 0$, the surface is hydrophobic. Conversely, $\Delta G_{sws} \geq 0$, the surface is hydrophilic.

Eqs. (4)–(6) only provide the information about interaction energy per unit area between two infinite planar surfaces. In order to get the actual interaction energy between the membrane (assumed to be an infinite planar surface) and sludge flocs (assumed to be a sphere), Derjaguin's approximation is used to indicate the total interaction energy between a flat sheet (membrane) and a sphere (sludge flocs) along the separation distance (d). According to the XDLVO theory, the total interaction energy (U_{swm}^{TOT}) can be given as the sum of Lifshitz–van der Waals (U^{LW}), Lewis acid–base (U^{AB}) and electrostatic double layer (U^{EL}) interactions:

$$U_{swm}^{TOT}(d) = U_{swm}^{LW}(d) + U_{swm}^{AB}(d) + U_{swm}^{EL}(d) \tag{10}$$

with

$$U_{swm}^{LW}(d) = 2\pi\Delta G_{d_0}^{LW}\frac{d_0^2 R}{d} \tag{11}$$

$$U_{swm}^{AB}(d) = 2\pi R\lambda\Delta G_{d_0}^{AB}\exp\left(\frac{d_0-d}{\lambda}\right) \tag{12}$$

$$U_{swm}^{EL}(d) = \pi\varepsilon_0\varepsilon_r R\left[2\xi_s\xi_m\ln\left(\frac{1+e^{-\kappa d}}{1-e^{-\kappa d}}\right)+\left(\xi_s^2+\xi_m^2\right)\ln\left(1-e^{-2\kappa d}\right)\right] \tag{13}$$

where R is the sludge flocs radius, and λ is the characteristic decay length of AB interactions in water (0.6 nm).

Similarly, the cohesion interaction energy with separation distance for sludge flocs–sludge flocs (U_{sws}^{TOT}) can be expressed as follows by the XDLVO theory (Brant and Childress, 2002):

$$U_{sws}^{TOT}(d) = U_{sws}^{LW}(d) + U_{sws}^{AB}(d) + U_{sws}^{EL}(d) \tag{14}$$

where $U_{sws}^{LW}(d)$, $U_{sws}^{AB}(d)$, and $U_{sws}^{EL}(d)$ can be again calculated by Eqs. (11)–(13). Correspondingly, the surface tension parameters of the membrane surface are replaced with sludge surface tension parameters as a result of the clean membrane surface being gradually covered with sludge flocs as the operating time proceeded.

1.3. Analytical methods

1.3.1. EPS extraction and analysis

The extraction of EPS from the sludge samples was based on the thermal treatment method (Hu et al., 2013). The extracts were analyzed for total carbohydrates and proteins, which were the dominant components in the extracted EPS (Bura et al., 1998). The modified Lowry method (Hartree, 1972) with bovine serum albumin (BSA) was used as the standard reference to determine the total concentration of proteins. The carbohydrate concentration was quantified using the phenol–sulfuric acid method (Dubois et al., 1956) with glucose as the standard reference. At least three measurements were conducted for each sample.

1.3.2. Contact angle measurement

The sludge layers were obtained by 0.45 μm acetate cellulose membranes which were washed three times with deionized water, and then placed on a 1% agar plate. After waiting for about 10 min to equilibrate the moisture between the agar and sludge layer, the contact angle was measured against ultrapure water, glycerol and diiodomethane by a contact angle meter (SL200A, Kono, USA) using the sessile drop technique (Hou et al., 2015). On the other hand, the new membrane was stored in ultrapure water at room temperature for 48 hr to remove impurities. The cleaned membrane was subsequently cut into smaller pieces and mounted on a glass slide with a double-sided adhesive. Before measurement, the membrane was air-dried for 24 hr. Similarly, the contact angles between the membrane and the three probe liquids as mentioned above were measured by the sessile drop approach (Tröger et al., 1997). For each sample, at least eight measurements at different locations were averaged to obtain the contact angle.

1.3.3. Zeta potential measurement

The sludge cells were equilibrated in 25 mL of 10 mmol/L NaCl solution (the concentration of 0.1 g SS/L) with its pH value pre-adjusted by 0.1 mol/L HCl and 0.1 mol/L NaOH solutions. After gentle agitation of the solution, the zeta potential of the sludge cells was measured at the desired pH values using a Malvern Nano ZS 90 (Malvern Instruments, UK) equipped with a dynamic light scattering device. Additionally, the zeta potential of the membrane was determined using a streaming potential analyzer (DelsaNano C/Solid Surface, Beckman, Germany) and calculated using the Helmholtz–Smoluchowski equation with the Fairbrother and Mastin substitution (Lin et al., 2014b). Each reported data value is an average of at least six measurements.

1.3.4. Other analyses

NH_3-N, NO_3-N, TN, TP, COD, MLSS, and MLVSS were measured according to Standard Methods (Chinese NEPA, 2002). The PSD of the sludge flocs was obtained using a laser granularity distribution analyzer (LS 230/SVM+, Beckman Coulter Corporation, USA) with a detection range of 0.4–2000 μm. The CST of different sludge samples was determined using a capillary suction timer (DPDFC-10A, China), and the normalized CST value was calculated by dividing the CST value by its MLSS concentration. Supernatant turbidity was measured with a turbidity meter (ET266020, Lovibond Corporation, Germany) after 30 min settling. Permeate turbidity was also measured with the aforementioned turbidity meter, pH with a pH meter (PHS-3C, China), DO concentration with a DO meter (Model HQ30d, Hach Corporation, USA), and the permeate flux of the DMBR with the volumetric method. The formed DM layer on the surface of the flat-sheet DM module was recorded by a digital SLR camera (SX260 HS, Canon Corporation, Japan).

2. Results and discussion

2.1. XDLVO prediction of sludge adhesion behaviors

As mentioned, the sludge adhesion behaviors on the membrane were mainly described by the interactions of membrane–sludge flocs. Table 2 lists the contact angles and zeta potentials of the nylon membrane and the three kinds of sludge samples, which are important data for the subsequent XDLVO calculations. Table 3 shows the calculated free energy of adhesion per unit area at contact for each membrane–sludge combination using Eqs. (4)–(6), (8) and (9). Significant differences were recorded for the adhesion free energies in the different membrane–sludge combinations, due to differences in the sludge properties. According to the XDLVO theory, a negative value of interaction energy between the membrane and sludge flocs signified attractive interactions, which facilitates the adhesion of sludge to the membrane. Conversely, a positive value indicated repulsive interaction, which resists adhesion of the sludge to

Table 2 – Contact angle and zeta potential of membrane and sludge samples.

Materials	Contact angle (°)			Zeta potential (mV) *
	Water	Glycerol	Diiodomethane	
Nylon mesh	102.32 ± 4.79	95.99 ± 3.77	31.89 ± 2.34	−46.50 ± 4.53
Sludge A	71.05 ± 1.30	70.47 ± 1.72	58.46 ± 1.04	−20.55 ± 1.79
Sludge B	67.08 ± 1.96	68.65 ± 2.51	63.29 ± 0.85	−21.45 ± 1.58
Sludge C	55.14 ± 3.08	62.27 ± 1.70	66.33 ± 1.71	−25.81 ± 1.17

* Values of zeta potential were measured in 0.01 mol/L NaCl solution at pH 7.7.

the membrane (Hong et al., 2013). As shown in Table 3, the negative values of ΔG_{swm}^{TOT} in all the membrane–sludge combinations indicated attractive interactions at contact between the nylon membrane and various sludge samples. Moreover, the lowest value of ΔG_{swm}^{TOT} recorded for the membrane–sludge A combination indicated the strongest level of sludge adhesion on the membrane. On the other hand, compared to $\Delta G_{d_0}^{LW}$ and $\Delta G_{d_0}^{EL}$, $\Delta G_{d_0}^{AB}$ contributed more to the ΔG_{swm}^{TOT} for all the membrane–sludge combinations. Therefore, the AB interaction is demonstrated to play an important role in the sludge adhesion process, which was similar with the results reported previously in the literatures (Brant and Childress, 2002; Hong et al., 2013).

Additionally, the values of ΔG_{sws} provided the quantitative degree of hydrophobicity/hydrophilicity of the solid surfaces. Many researchers have applied this parameter to assess the hydrophobicity/hydrophilicity of sludge flocs, cellulose acetate membrane, microalgae and so on (Ahmad et al., 2013; Hong et al., 2013; Su et al., 2013). A positive value of ΔG_{sws} signified a hydrophilic surface while a negative value indicated a hydrophobic surface. Among the three sludge types, sludge A was more hydrophobic than sludge B, whereas sludge C was the hydrophilic. The hydrophobicity/hydrophilicity of sludge may be affected by other sludge properties such as EPS, further discussion of which is presented in Section 2.5.

The profiles of the interaction energies at the different separation distances for the various membrane–sludge combinations were respectively calculated using Eqs. (10)–(13) and depicted in Fig. 2. Fig. 2 demonstrates that EL interaction was repulsive while LW and AB interactions were attractive. Furthermore, the interaction energies decreased to almost zero along with the increase of the separation distance. Consequently, adhesion of all the sludge flocs to the membrane surface first encountered an attractive secondary energy minimum at a long separation distance (25.7–30.0 nm). Subsequently, the sludge flocs went through a significant repulsive energy barrier at a short separation distance (3.4–3.9 nm). The secondary energy minimum signified the ability of the sludge flocs to adsorb onto the membrane surface, which represented a reversible adhesion (Redman et al., 2004). In other words, the sludge flocs more readily desorbed from the membrane surface as the absolute value of the secondary energy minimum decreased. On the other hand, the energy barrier indicated the required kinetic energy for the dispersed sludge flocs in suspension to overcome the barrier to reach the membrane surface (Hoek et al., 2003). It was demonstrated that a higher energy barrier more strongly resists the sludge adhesion to the membrane surface.

Moreover, it appeared that the value of the energy barrier was several orders of magnitude higher than that of the secondary energy minimum. So, the resistance effect at the energy barrier was more significant than the reversible adhesion effect at the secondary energy minimum during the sludge adhesion process. Therefore, through the results of the energy barrier illustrated in Fig. 2 (1934.3, 2159.4 and 3014.1 kT for the sludge A–, sludge B–, sludge C–membrane combination, respectively), it is expected that sludge A would adhere more quickly to the membrane surface and complete the sludge adhesion process in the DMBR than sludge B and sludge C. In contrast, sludge C would adhere to the membrane surface slower than the other two sludge samples due to the higher repulsive energy barrier.

2.2. XDLVO prediction of sludge cohesion behaviors

As noted earlier, following the initial adhesion of sludge flocs to the membrane surface, the adhesion interactions of membrane–sludge flocs are mostly overtaken by the cohesion interactions of sludge flocs–sludge flocs. Table 4 shows the calculated cohesion free energy per unit area at contact for the various sludge floc–sludge floc combinations. It was found that AB interaction was more important in the sludge cohesion process than LW and EL interactions. Referring to the significances of the positive and negative interaction energy in Section 2.1, the positive value of ΔG_{sws}^{TOT} in the sludge C–sludge C combination indicated that the sequential cohesion of sludge C encountered resistance when the deposited sludge flocs initially formed a sludge layer on the membrane surface, which was against the DM layer formation. Conversely, the negative values of ΔG_{sws}^{TOT} in the sludge A–sludge A and sludge B–sludge B combinations signified the attractive effect during the cohesion of sludge flocs on the sludge layer formed, which facilitated the continuous cohesion of sludge flocs. Moreover, the stronger level of attraction in sludge A–sludge A than in sludge B and sludge B indicated that sludge A more readily forms a DM layer than sludge B.

Fig. 3 illustrates the profiles of interaction energies with separation distances for the various sludge floc–sludge floc combinations. Overall, the evolution trends of TOT, LW, AB, and EL interaction energies observed in Fig. 3a and b were similar to those of Fig. 2a and b. However, there were significant changes in the values. For instance, the secondary energy minimum changed from –19.0 and –11.7 kT to –3.7 and –1.4 kT, while the energy barrier significantly decreased from 1934.3 and 2159.4 kT to 476.3 and 657.4 kT for sludge A–sludge A and sludge B–sludge B, respectively. These results show that the initial sludge adhesion facilitates the following sludge cohesion due to the remarkable reduction of the repulsive energy barrier (Hong et al., 2013).

Importantly, sludge A was subject to a lower repulsive interaction (U^{EL}) than sludge B, resulting in a lower energy barrier during the sludge cohesion process, which might promote the DM layer formation in the DMBR. But in the case of sludge C–sludge C, significantly different interaction energy is observed as shown in Fig. 3c. Here, the AB interaction was repulsive, in contrast to the attractive interaction as shown in Fig. 2c. Consequently, there was no noticeable energy barrier

Table 3 – Adhesion free energies (mJ/m^2) at contact between the membrane and the various sludge samples.

	Materials	$\Delta G_{d_0}^{LW}$	$\Delta G_{d_0}^{AB}$	$\Delta G_{d_0}^{EL}$	ΔG_{swm}^{TOT}	ΔG_{sws}
Nylon mesh–sludge flocs	Sludge A	–2.91	–42.44	–1.24	–46.59	–17.88
	Sludge B	–1.91	–37.38	–1.13	–40.41	–7.28
	Sludge C	–1.25	–27.01	–0.65	–28.91	14.29

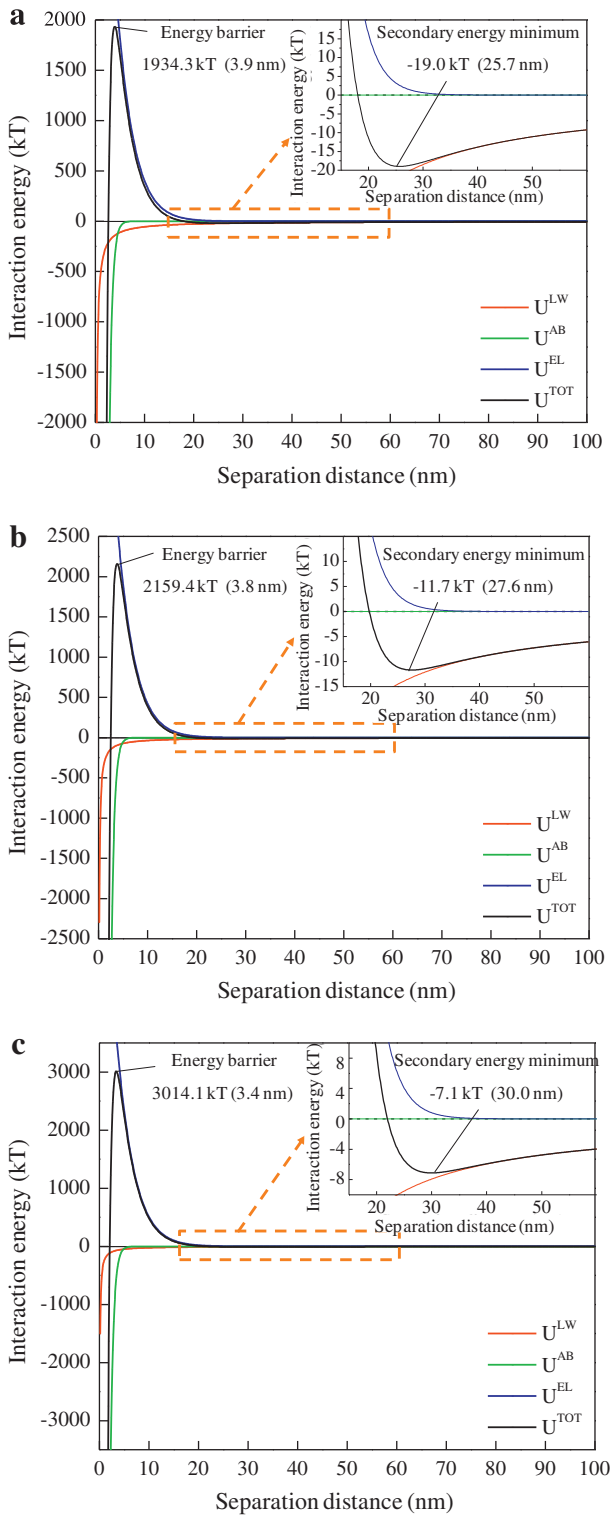

Fig. 2 – Profiles of Lifshitz–van der Waals (LW), Lewis acid–base (AB), electrostatic double layer (EL) and total (TOT) interaction energies with separation distance between membrane and (a) sludge A, (b) sludge B, and (c) sludge C.

and the secondary energy minimum was only −0.53 kT on the U^{TOT} curve, which indicated a weak reversible adhesion at the secondary energy minimum. Compared to sludge A and sludge B, sludge C suffered a greater repulsive interaction during the cohering of sludge flocs to the surface of the deposited sludge flocs, which might delay the DM layer formation in the DMBR. Overall, the variations in cohesion interaction energies in the different sludge floc–sludge floc combinations further highlight the distinct properties of the various sludge samples.

2.3. Filtration performance of sludge flocs

The filtration tests were carried out within 240 min for the three different sludge samples to investigate the DM formation performance under constant pressure mode. In DMBRs the filtration resistance was much lower (~10^{10} m^{-1}), even under constant pressure mode the flux could keep at high values for a long operation cycle of 3–5 days as reported previously (Hu et al., 2017). However, in MBRs the filtration resistances (~10^{12} m^{-1}) were quite high, using constant pressure mode the decline of flux would be serious and normal filtration flux could not be sustained. Thus in real application of MBR constant flux modes were always used, while in DMBR studies both operation modes were adopted without paying much attention to the sustainability of filtration process.

In DMBRs, the permeate flux and turbidity are the important indicators used to describe the filtration performance of the DM layer (Hu et al., 2016; Liang et al., 2013), which are shown in Fig. 4. From Fig. 4a, all the sludge samples were subject to higher turbidity (28.2–1000 NTU) at t = 0 due to the insufficient rejection of fine particles in the sludge flocs by the large pore material itself. Subsequently, the quick adhesion of sludge flocs onto the surface and into the pores of the mesh membrane caused the sharp decline of turbidity in the initial filtration period.

The formation of the DM layer was quantitatively described by considering a decrease in turbidity below 1 NTU as an indicator for the initial formation of the DM layer (Hu et al., 2016). Fig. 4a shows that the initial DM formation time for sludge A and sludge B was approximately 50 and 60 min, respectively. Conversely, the turbidity of sludge C remained above 1 NTU, indicating that the initial formation of the DM layer was extremely slow (>240 min). At the DM maturation stage, the DM layer was continuously consolidated with a corresponding increase in the rejection capacity of the DM layer, which significantly lowered the turbidity to provide a rough indicator for the DM maturation. The average turbidity at this stage was 0.69 (50–240 min), 0.92 (60–240 min) and 2.70 NTU (90–240 min) for sludges A, B and C, respectively. Here, the turbidity of slightly higher than 1 NTU was observed for sludge C, which, however, approximately remained stable for 90–240 min.

As shown in Fig. 4b, under constant pressure operation by gravity flow (10-cm water head), a dramatic flux decline was recorded at the initial DM formation stage. Subsequently, the flux decline was more gradual at the DM maturation stage and ended at the flux of *circa* 96 L/(m^2·hr) for sludge A. A similar evolution trend of flux was observed for sludge B, although a higher flux (177 L/(m^2·hr)) was achieved at the end of the operation. Overall, the flux of sludge A declined by almost 45% within 20 min of the filtration time, which was higher than that of 30% for sludge B in the same filtration timeframe. But for sludge C, a relatively gentle flux decline was obtained during the whole filtration period, which ended at 115 L/(m^2·hr). In general, the variations in permeate flux and turbidity during filtration

Table 4 – Cohesion free energy (mJ/m^2) at contact between the various sludge flocs-sludge flocs.

	Materials	$\Delta G_{d_0}^{LW}$	$\Delta G_{d_0}^{AB}$	$\Delta G_{d_0}^{EL}$	ΔG_{sws}^{TOT}
Sludge flocs–sludge flocs	Sludge A	−1.15	−16.72	0.10	−17.78
	Sludge B	−0.49	−6.79	0.10	−7.18
	Sludge C	−0.21	14.50	0.15	14.44

were distinct for the various sludge samples in the DMBR mostly due to the differences in the sludge properties.

Furthermore, observations of the various DM layers at the end of the filtration time are recorded in Fig. 5. It was evident that the DM layer of sludge C was more easily detached from the membrane surface than those of sludge A and sludge B when the DM modules were removed from the bioreactor. The DM layers of sludge A and sludge B seemed to be more integrated and uniform than that of sludge C. This finding further confirmed that the sludge C was loosely attached to the membrane surface and was relatively difficult to form a DM layer within a short time.

Additionally, it is worth noting that our experiment was operated under gravity filtration mode. Ten centimeters of water head is equivalent to 1 kPa transmembrane pressure (TMP), which acted as the driving force for effluent production. It is the fact that different TMP will result in the varied driving force, filtration flux and formation time, thus in DMBR the particles and other foulants that could attach on the mesh surface would be different in size when other operation conditions were the same. As such, the formed DM layer would show different morphologies, components and structures as well as short-term and long-term filtration performance, thus more work should be done about the effect of TMP on adhesion of sludge on the support material in the future.

2.4. *Feasibility of predicting DM layer formation by XDLVO theory*

Table 5 summarizes the results of various interaction energies by XDLVO prediction and practical filtration. In the XDLVO prediction of the sludge adhesion process, the attractive interaction energies (ΔG_{swm}^{TOT}) between the membrane and sludge flocs decreased in the following order: sludge A > sludge B > sludge C. Moreover, the energy barrier and secondary energy minimum both increased in the following order: sludge A < sludge B < sludge C. These results indicated that the adhesion tendencies of sludges A, B, and C on the membrane surface were high, moderate, and low, respectively, which supported the results of the initial DM formation time in the practical filtration tests. Therefore, it could be concluded that a higher predicted adhesion tendency of membrane–sludge flocs indicates a shorter initial DM formation time in DMBRs.

Similarly, in the XDLVO prediction of the sludge cohesion process, the cohesion tendencies of the various sludge floc–sludge floc combinations were similar to the adhesion tendencies of membrane–sludge floc combinations. Nonetheless, the ΔG_{sws}^{TOT} of sludge C was repulsive, and the energy barrier was non-existent. In the practical DMBR filtration, it was general to comprehensively evaluate the indicators of permeate turbidity and flux for all the DMBR operational stages. However, at the DM layer formation stage much more attention should be paid to the indicator of turbidity in the acceptable range of permeate flux (such as 96–177 L/(m^2·hr) in this study). As a result, the cohesion tendencies obtained by the XDLVO prediction were considered to corroborate with the turbidity results of the DM maturation stage obtained during the practical filtrations. These findings proved that the XDLVO theory could provide useful information for predicting the DM layer formation in the DMBR.

Additionally, the AB interaction was a main contributor to the ΔG_{swm}^{TOT} and ΔG_{sws}^{TOT} due to its high proportion, and which was calculated based on the electron acceptor (γ^+) and electron donor components (γ^-) of the sludge flocs that were mainly affected by the pH and ionic strength of the sludge suspension (Wang et al., 2013b; Zhang et al., 2014). The changes of pH and ionic strength resulted in the variations of AB interaction. A previous MBR study showed that in the range of neutral–alkaline conditions (pH = 6.5–9.0) the increment of ionic strength (5–150 mM NaCl) could facilitate the attachment of foulants to membrane surfaces (Wang et al., 2013b). However, in the DMBR, the effects of ionic strength and pH on the formation of the DM layer need further study. Moreover, from Table 5, it was clear that the energy barrier and secondary energy minimum were also essential to determine the interactions of sludge adhesion and cohesion process.

2.5. *Effects of sludge properties on the DM layer formation*

As previously noted above, sludge properties played an important role in the DM layer formation in DMBRs. The sludge properties (Table 1) can approximately be classified into five categories, namely, EPS (EPS_p, EPS_c, EPS_{tot}), morphology (PSD), settleability (SVI), dewaterability (CST and normalized CST), and flocculability (supernatant turbidity) (Chen et al., 1996; Hu et al., 2017; Huang et al., 2012; Sun et al., 2007). Overall, the dominant properties of sludge A were poor settleability and dewaterability (with higher SVI, CST, and normalized CST values). Sludge C showed poor flocculability (with higher supernatant turbidity), whereas sludge B showed relatively normal properties than the others. According to the practical filtration results reported in Section 2.3, sludge B showed a more acceptable DM formation performance (such as short initial DM formation time, low permeate turbidity, and high permeate flux) than sludge A and sludge C.

EPS is considered to be a key biological substance that determines sludge hydrophobicity and other properties (Lin et al., 2014a). Notably, the proteins in EPS (EPS_p) are considered to influence the sludge hydrophobicity significantly than the carbohydrates in EPS (EPS_c) because of the aromatic or aliphatic side chains of amino acids. In other words, sludge hydrophobicity increases with EPS_p content (Hong et al., 2013), which was theoretically confirmed by ΔG_{sws} in Section 2.1 (hydrophobicity was sludge A > sludge B > sludge C). The sludge with higher hydrophobicity more readily deposited on the membrane surface to form the cake layer (Su et al., 2013), resulting in the undesirable cake layer fouling in MBRs. Conversely, in the DMBR, the adherence of substances (cake layer) on the support mesh during the initial filtration stage is necessary and desired. Unlike the order of sludge hydrophobicity, the initial DM formation time was in the order of sludge A < sludge B < sludge C. Therefore, EPS_p further affected the adhesion process of sludge flocs on the membrane surface, in this study, which corroborated the findings of Hong et al. (2013).

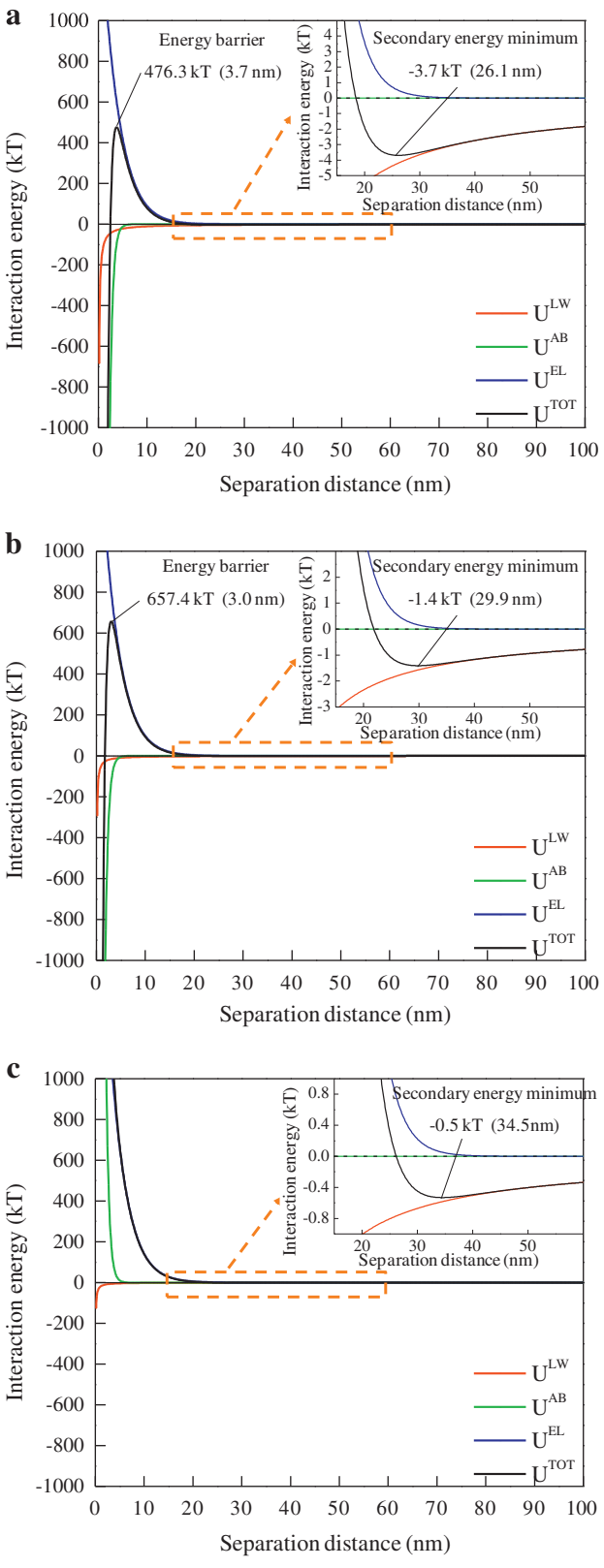

Fig. 3 – Profiles of Lifshitz–van der Waals (LW), Lewis acid–base (AB), electrostatic double layer (EL) and total (TOT) interaction energies with separation distance for (a) sludge A–sludge A, (b) sludge B–sludge B, and (c) sludge C–sludge C.

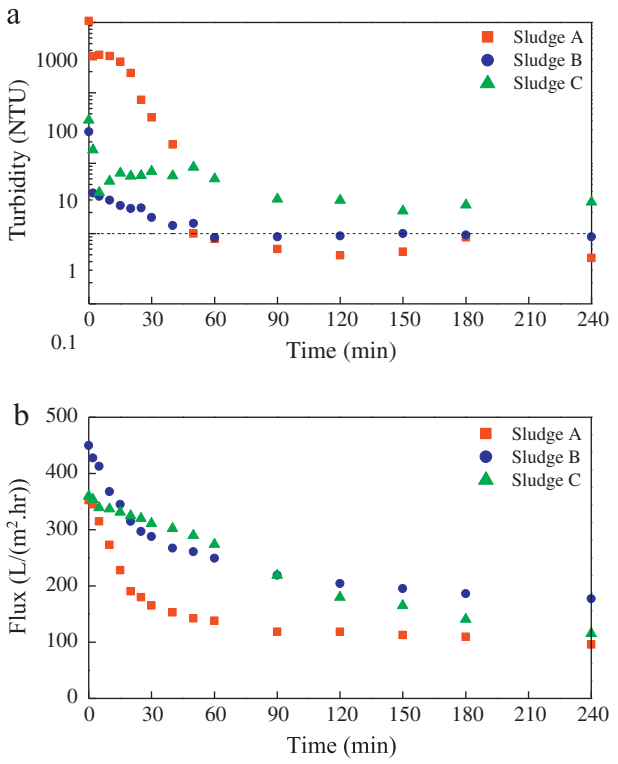

Fig. 4 – Comparison of filtration performance of dynamic membrane (DM): (a) permeate turbidity, and (b) permeate flux.

For the sludge morphology (PSD), it is reported that large particles in the sludge suspension appeared to accelerate the formation of the DM layer in the DMBR system, contrary to the preferential accumulation of smaller particles on the membrane surface in MBR systems (Hu et al., 2016). However, in this study, the DM layer formation by sludge C with larger particles (PSD = 60.41 μm) but poor flocculability (supernatant turbidity = 31.70 NTU) was slower (more than 240 min). Thus, the poor flocculability apparently weakened the influence of particle size on the DM formation process. As reported, sludge flocculability could be adequately explained by the XDLVO theory (Li et al., 2014). Therefore, from the interaction point of view, the repulsive interactions between particles were predominant in sludge C as shown in Table 4 (ΔG_{sws}^{TOT}) and Fig. 3c (U^{TOT}). Repulsive interactions between particles caused the particles to repel each other and to remain in the discrete and single status, which readily impeded flocculability in the sludge (Lin et al., 2014a). Moreover, the high energy barrier and secondary energy minimum in the U^{TOT} curve as shown in Figs. 2c and 3c (no energy barrier but high repulsive interaction) indicated that the sludge with poor flocculability exerted a negative impact on the DM layer formation in the DMBR.

It is reported that the sludge dewaterability and settleability are affected by many factors, among which the EPS concentration and structure are most important (Chen et al., 2001; Fan et al., 2015). In this study, sludge A showed comparatively poor dewaterability and settleability possibly due to the high extracellular polymers (such as EPS) associated with secretions by

Fig. 5 – Pictures of DM module: (a) new membrane, (b) DM layer of sludge A, (c) DM layer of sludge B, and (d) DM layer of sludge C.

filamentous bacteria and/or other microbes (Houghton et al., 2001; Meng et al., 2006b). EPS could further affect the porosity and structure of the DM layer (Kim et al., 1998), which resulted in some influence on the DM performance. Moreover, sludge A was considered to be a bulking sludge, because more filamentous bacteria were observed in sludge A through the microscopic observation. Irregular filamentous bacteria themselves could wrap and fix the foulants to the surface of the support material, which might contribute to the fast formation of DM in the initial filtration stage as compared with the other sludges. In addition, according to the XDLVO theory, sludge A had the strongest attractive interaction when the sludge flocs attached to the membrane surface and on the deposited sludge flocs (ΔG_{swm}^{TOT} in Table 3 and ΔG_{sws}^{TOT} in Table 4). On the other hand, the low energy barrier and secondary energy minimum in the U^{TOT} curve shown in Figs. 2a and 3a indicated that the sludge with poor settleability and dewaterability accelerated the DM layer formation as evidenced by the short time (50 min) used for the initial DM formation. Unfortunately, the sludge with poor settleability and dewaterability induced high filtration resistance and low permeate flux in the DMBR, which was in agreement with previous findings reported for MBRs (Meng et al., 2006a).

3. Conclusion

Theoretical and experimental analyses were carried out to elucidate the effects of sludge properties on the DM layer formation. XDLVO calculations showed that AB interaction was a key determinant of the adhesion energy of membrane–sludge

Table 5 – Results of XDLVO prediction and practical filtration test.

Sample	XDLVO prediction				Practical filtration	
	Adhesion process				Initial DM formation time (min)	Comments
	ΔG_{swm}^{TOT} (mJ/m^2)	EB [a] (kT)	SEM [b] (kT)	Adhesion tendency		
Sludge A	-46.6	1934.3	-19.0	High	50	High adhesion tendency predicts short DM formation time
Sludge B	-40.4	2159.4	-11.7	Moderate	60	
Sludge C	-28.9	3014.1	-7.1	Low	>240	
Sample	Cohesion process				Turbidity [c] (NTU)	Comments
	ΔG_{sws}^{TOT} (mJ/m^2)	EB (kT)	SEM (kT)	Cohesion tendency		
Sludge A	-17.8	476.3	-3.7	High	0.69	High cohesion tendency predicts low turbidity
Sludge B	-7.2	657.4	-1.4	Moderate	0.92	
Sludge C	14.4	– [d]	-0.5	Low	2.70	

XDLVO: extended Derjaguin–Landau–Verwey–Overbeek; DM: dynamic membrane.
[a] Energy barrier.
[b] Secondary energy minimum.
[c] Average turbidity at the DM maturation stage.
[d] Energy barrier was non-existent in the total interaction energy curve during the sludge cohesion process, and total interaction energy was all positive value within 26 nm separation distance between sludge flocs and sludge flocs.

flocs and cohesion energy of sludge flocs–sludge flocs. Furthermore, proper control of the energy barrier and secondary energy minimum enhanced the sludge adhesion and cohesion processes. Filtration results adequately validated predictions of the DM layer formation by the XDLVO theory. Evidently, positive modifications to the sludge properties (such as EPS, settleability, dewaterability, and flocculability) were essential to enhance the DM layer formation. Therefore, the feasibility of predicting the DM formation process with the XDLVO theory is hereby validated, which proves useful for the optimization of sludge properties and/or operational parameters to facilitate the stable operation of DMBR systems.

Acknowledgments

This work was supported by the National Natural Science Foundation of China (Nos. 51778522, and 51508450), the Science Foundation for Fostering Talents of Xi'an University of Architecture and Technology (No. RC1710), and the Program for Innovative Research Team in Shaanxi (No. IRT2013KCT-13).

Appendix A. Supplementary data

Supplementary data to this article can be found online at https://doi.org/10.1016/j.jes.2018.06.017.

REFERENCES

Ahmad, A.L., Yasin, N.H.M., Derek, C.J.C., Lim, J.K., 2013. Harvesting of microalgal biomass using MF membrane: kinetic model, CDE model and extended DLVO theory. J. Membr. Sci. 446 (11), 341–349.

Bouchard, C.R., Jolicoeur, J., Kouadio, P., Britten, M., 1997. Study of humic acid adsorption on nanofiltration membranes by contact angle measurements. Can. J. Chem. Eng. 75 (2), 339–345.

Brant, J.A., Childress, A.E., 2002. Assessing short-range membrane–colloid interactions using surface energetics. J. Membr. Sci. 203 (1–2), 257–273.

Bura, R., Cheung, M., Liao, B., Finlayson, J., 1998. Composition of extracellular polymeric substances in the activated sludge floc matrix. Water Sci. Technol. 37 (4), 325–333.

Cai, X., Zhang, M., Yang, L., Lin, H., Wu, X., He, Y., et al., 2017. Quantification of interfacial interactions between a rough sludge floc and membrane surface in a membrane bioreactor. J. Colloid Interface Sci. 490, 710–718.

Chen, G.W., Lin, W.W., Lee, D.J., 1996. Capillary suction time (CST) as a measure of sludge dewaterability. Water Sci. Technol. 34 (96), 443–448.

Chen, Y., Yang, H., Gu, G., 2001. Effect of acid and surfactant treatment on activated sludge dewatering and settling. Water Res. 35 (11), 2615–2620.

Chinese NEPA, 2002. Water and Wastewater Monitoring Methods. Chinese Environmental Science Publishing House, Beijing, China.

Dubois, M., Gilles, K.A., Hamilton, J.K., Rebers, P.A., Smith, F., 1956. Colorimetric method for determination of sugars and related substances. Anal. Chem. 28 (3), 350–356.

Fan, B., Huang, X., 2002. Characteristics of a self-forming dynamic membrane coupled with a bioreactor for municipal wastewater treatment. Environ. Sci. Technol. 36 (23), 5245–5251.

Fan, L., Zhou, Q., Wu, D., Wang, T., Shao, L., He, P., 2015. Dewaterability of anaerobic digestate from food waste: relationship with extracellular polymeric substances. Chem. Eng. J. 262, 932–938.

Hartree, E.F., 1972. Determination of protein: a modification of the Lowry method that gives a linear photometric response. Anal. Biochem. 48 (2), 422–427.

Hoek, E.M.V., Bhattacharjee, S., Elimelech, M., 2003. Effect of membrane surface roughness on colloid–membrane DLVO interactions. Langmuir 19 (11), 4836–4847.

Hong, H., Peng, W., Zhang, M., Chen, J., He, Y., Wang, F., et al., 2013. Thermodynamic analysis of membrane fouling in a submerged membrane bioreactor and its implications. Bioresour. Technol. 146 (10), 7–14.

Hou, X., Liu, S., Zhang, Z., 2015. Role of extracellular polymeric substance in determining the high aggregation ability of anammox sludge. Water Res. 75, 51–62.

Houghton, J.I., Quarmby, J., Stephenson, T., 2001. Municipal wastewater sludge dewaterability and the presence of microbial extracellular polymer. Water Sci. Technol. 44 (2–3), 373–379.

Hu, Y., Wang, X.C., Zhang, Y., Li, Y., Chen, H., Jin, P., 2013. Characteristics of an A^2O–MBR system for reclaimed water production under constant flux at low TMP. J. Membr. Sci. 431 (431), 156–162.

Hu, Y., Wang, X.C., Tian, W., Ngo, H.H., Chen, R., 2016. Towards stable operation of a dynamic membrane bioreactor (DMBR): operational process, behavior and retention effect of dynamic membrane. J. Membr. Sci. 498, 20–29.

Hu, Y., Wang, X.C., Sun, Q., Ngo, H.H., Yu, Z., Tang, J., et al., 2017. Characterization of a hybrid powdered activated carbon-dynamic membrane bioreactor (PAC-DMBR) process with high flux by gravity flow: operational performance and sludge properties. Bioresour. Technol. 223, 65–73.

Huang, J.S., Wen, Y., Cao, A.S., Li, H.S., Zhou, Q., 2012. The influence of temperature on bioflocculation and settling of activated sludge and their flocculation mechanisms involved. Adv. Mater. Res. 518-523, 1817–1824.

Kim, J.S., Lee, C.H., Chun, H.D., 1998. Comparison of ultrafiltration characteristics between activated sludge and BAC sludge. Water Res. 32, 3443–3451.

Kuberkar, V.T., Davis, R.H., 2000. Modeling of fouling reduction by secondary membranes. J. Membr. Sci. 168 (1), 243–258.

Li, H., Wen, Y., Cao, A., Huang, J., Zhou, Q., 2014. The influence of multivalent cations on the flocculation of activated sludge with different sludge retention times. Water Res. 55 (2), 225–232.

Liang, S., Qu, L., Meng, F., Han, X., Zhang, J., 2013. Effect of sludge properties on the filtration characteristics of self-forming dynamic membranes (SFDMs) in aerobic bioreactors: formation time, filtration resistance, and fouling propensity. J. Membr. Sci. 436 (2), 186–194.

Lin, H., Zhang, M., Wang, F., Meng, F., Liao, B.Q., Hong, H., et al., 2014a. A critical review of extracellular polymeric substances (EPSs) in membrane bioreactors: characteristics, roles in membrane fouling and control strategies. J. Membr. Sci. 460 (9), 110–125.

Lin, T., Lu, Z., Chen, W., 2014b. Interaction mechanisms and predictions on membrane fouling in an ultrafiltration system, using the XDLVO approach. J. Membr. Sci. 461, 49–58.

Meng, F., Yang, F., Xiao, J., Zhang, H., Gong, Z., 2006a. A new insight into membrane fouling mechanism during membrane filtration of bulking and normal sludge suspension. J. Membr. Sci. 285 (1–2), 159–165.

Meng, F., Zhang, H., Yang, F., Li, Y., Xiao, J., Zhang, X., 2006b. Effect of filamentous bacteria on membrane fouling in submerged membrane bioreactor. J. Membr. Sci. 272, 161–168.

Ouyang, K., Liu, J., 2009. Effect of sludge retention time on sludge characteristics and membrane fouling of membrane bioreactor. J. Environ. Sci. 21 (10), 1329–1335.

Park, M.S., Kiso, Y., Jung, Y.J., Simase, M., Wang, W.H., Kitao, T., et al., 2004. Sludge thickening performance of mesh filtration process. Water Sci. Technol. 50 (8), 125–133.

Redman, J.A., Walker, S.L., Elimelech, M., 2004. Bacterial adhesion and transport in porous media: role of the secondary energy minimum. Environ. Sci. Technol. 38 (6), 1777–1785.

Shen, L.G., Lei, Q., Chen, J.R., Hong, H.C., He, Y.M., Lin, H.J., 2015. Membrane fouling in a submerged membrane bioreactor: impacts of floc size. Chem. Eng. J. 269, 328–334.

Su, X., Tian, Y., Li, H., Wang, C., 2013. New insights into membrane fouling based on characterization of cake sludge and bulk sludge: an especial attention to sludge aggregation. Bioresour. Technol. 128 (1), 586–592.

Sun, Y., Yong, W., Xia, H., 2007. Relationship between sludge settleability and membrane fouling in a membrane bioreactor. Front. Environ. Sci. Eng. 1 (2), 221–225.

Tröger, J., Lunkwitz, K., Bürger, W., 1997. Determination of the surface tension of microporous membranes using contact angle measurements. J. Colloid Interface Sci. 194 (2), 281–286.

van Oss, C.J.V., 1995. Hydrophobicity of biosurfaces — origin, quantitative determination and interaction energies. Colloids Surf. B: Biointerfaces 5 (3–4), 91–110.

van Oss, C.J.V., 2003. Long-range and short-range mechanisms of hydrophobic attraction and hydrophilic repulsion in specific and aspecific interactions. J. Mol. Recognit. 16 (4), 177–190.

van Oss, C.J.V., Good, R.J., 1988. Orientation of the water molecules of hydration of human serum albumin. Protein J. 7 (2), 179–183.

van Oss, C.J.V., Good, R.J., Chaudhury, M.K., 1986. The role of van der Waals forces and hydrogen bonds in "hydrophobic interactions" between biopolymers and low energy surfaces. J. Colloid Interface Sci. 111 (2), 378–390.

Wang, L., Miao, R., Wang, X., Lv, Y., Meng, X., Yang, Y., et al., 2013a. Fouling behavior of typical organic foulants in polyvinylidene fluoride ultrafiltration membranes: characterization from microforces. Environ. Sci. Technol. 47 (8), 3708–3714.

Wang, Q., Wang, Z., Zhu, C., Mei, X., Wu, Z., 2013b. Assessment of SMP fouling by foulant–membrane interaction energy analysis. J. Membr. Sci. 446, 154–163.

Yu, Y., Yang, Z., Duan, Y., 2017. Structure and flow calculation of cake layer on microfiltration membranes. J. Environ. Sci. 56 (6), 95–101.

Zhang, X., Wang, Z., Wu, Z., Wei, T., Lu, F., Tong, J., et al., 2011. Membrane fouling in an anaerobic dynamic membrane bioreactor (AnDMBR) for municipal wastewater treatment: characteristics of membrane foulants and bulk sludge. Process Biochem. 46 (8), 1538–1544.

Zhang, Y., Zhang, M., Wang, F., Hong, H., Wang, A., Wang, J., et al., 2014. Membrane fouling in a submerged membrane bioreactor: effect of pH and its implications. Bioresour. Technol. 152, 7–14.